

Variode Enabled Frequency-Reconfigurable Microstrip Patch Antenna with Operation Band Covering S and C Bands

Caibiao Guo¹, Lianwen Deng¹, Jian Dong², Tulin Yi³, Congwei Liao¹,
Shengxiang Huang¹, and Heng Luo^{1,*}

Abstract—A frequency continuous reconfigurable microstrip patch antenna with operation band covering S-band and C-band is introduced. The antenna consists of a central rectangular patch and four parasitic patches with a symmetrical structure, connected by four varactor diodes in the middle position of the edge of each patch. With help of HFSS microwave studio simulation, results have shown that, by altering the bias voltage on varactor diodes, the operated frequencies vary continuously within a wide range from 3.29 to 4.01 GHz and 5.35 to 7.00 GHz, which cover S-band and C-band. Further measurement, which verifies the simulation by reasonable agreement, has been carried out. Besides, this frequency reconfigurable antenna maintains broadside radiation and stable radiation pattern. Specifically, the gain is basically maintained at around 4.5 dBi with the working frequency increasing from 3.60 to 7.00 GHz. Compared with other frequency-reconfigurable antennas available in previous literature, the proposed antenna has advantages of a wide frequency tuning range, high frequency selectivity, simple and stable structure, low cost, and miniaturization, which make it a promising candidate as cognitive radio and future wireless communication systems.

1. INTRODUCTION

With the rapid advancement in wireless communication technologies [1–4], the demand for multi-band mobile devices [5, 6] is increasing. For example, the current wireless transceivers have to support various communication protocols such as LTE, WiMAX, and WLAN, simultaneously. Each of these technologies operates at a different frequency band. Therefore, instead of using several antennas, it is more compact and efficient to use one multi-band antenna that accommodates multiple modes. A reconfigurable antenna [7–14] is an antenna capable of dynamically modifying its frequency and radiation properties in a controlled and reversible manner in order to provide a dynamical response. By using different patch reconfigurations we obtain different results of gain, bandwidth, and efficiency.

Several approaches have been followed in regards of designing multi-band antennas. The frequency reconfigurable microstrip antenna changes structure and current distribution by loading one or more electronic control components. Therefore, in order to ensure the communication system stability [15], antennas with tunable resonant frequency while other parameters remain substantially unchanged [16] are urgently needed. With the aims at tunable operation model, switches including RF MEMS [17], and PIN diodes, varactor diodes [18], lumped elements and electronic radio frequency (RF) switching devices [19] are commonly used to design electrical frequency reconfigurable antennas [20]. In spite of great breakthrough toward frequency-tunable property, these strategies still suffer from some drawbacks. For example, the RF MEMS' drawbacks are lower reliability, slower response speed, higher cost than

Received 2 November 2019, Accepted 30 December 2019, Scheduled 16 January 2020

* Corresponding author: Heng Luo (luohengcsu@csu.edu.cn).

¹ School of Physics and Electronics, Central South University, Changsha 410083, China. ² School of Computer Science and Engineering, Central South University, Changsha 410083, China. ³ Department of Basics, Air Force Early Warning Academy, Wuhan 430019, China.

PIN diodes [21] and varactor diodes. Various frequency reconfigurable microstrip patch antennas have been reported previously, because they feature miniaturization, ease of manufacture, and fast response [22, 23]. Majid et al. [24] demonstrated that the resonant frequency can be reconstructed between multiple discrete bands by adding five PIN diodes switches under a slot of the patch. Chattha et al. [4] presented a compact printed multi-band frequency reconfigurable patch antenna by inserting three PIN diodes. However, due to the turn-on and turn-off characteristics of PIN diodes, there only exist two kinds of operation model in the PIN diodes enabled system, leading to that the resonant frequency cannot be tuned continuously. Cai et al. [25] and Tateno et al. [26] demonstrated that the operating frequency of the antenna containing two varactor diodes is continuously adjustable from 2.45 ~ 3.55 GHz and 3.5 ~ 3.9 GHz respectively by changing the bias voltage. However, those reconfigurable antennas can be tuned in only one frequency band (S-band), and the tunable bandwidth is urgently needed to be broadened.

In this paper, a compact ($33.9 \times 38 \times 1.6 \text{ mm}^3$) frequency continuous reconfigurable microstrip antenna switching between S-band (2 ~ 4 GHz) and C-band (4 ~ 8 GHz) with coaxial single point feed is proposed. Due to the higher response speed and continuity than PIN diodes, varactor diodes are used in the simulation environment (HFSS) to achieve tunable capacitance, which is responsible for frequency reconfigurability. It seems that the two groups of varactor diodes in the symmetrical structure changed separately to stimulate two working modes, and the resonant frequency of the antenna can be continuously tuned in a wide range from 3.29 ~ 4.01 GHz and 5.35 ~ 7.00 GHz. At the same time, the whole structure of the antenna remains basically unchanged with the adjustment of capacitance so that the unidirectional radiation pattern of the antenna remains substantially constant within the tunable range, leading to a stable gain approximately around 4.5 dBi. Meanwhile, a very simple DC bias circuit is designed to control the capacitance of the varactor diodes for tuning the resonant frequency. A prototype of the designed antenna is fabricated and measured to validate simulation results. The proposed reconfigurable antenna demonstrates a reasonable agreement between the measured and simulated results. The above study provides a new research idea for broadening the tunable bandwidth of frequency-reconfigurable microstrip patch antenna.

2. RECONFIGURABLE ANTENNA DESIGN

2.1. The Geometry of the Proposed Antenna

As shown in Figure 1, the layout of the proposed antenna includes radiation patches, rectangular substrate, and the ground. Lumped elements are used in the simulation environment to achieve tunable

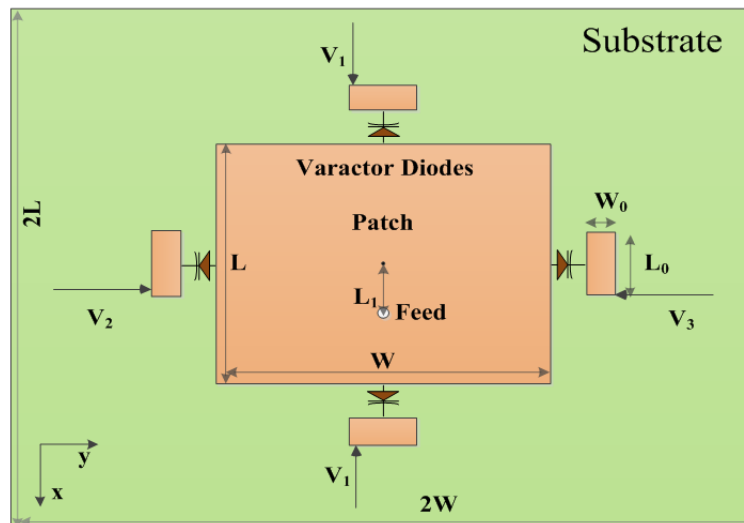


Figure 1. The structure of the proposed reconfigurable antenna.

capacitance, which is responsible for frequency reconfigurability. The sizes of substrate along both X and Y directions are twice as large as that of the center patch. Note that four identical parasitic patches are designed around the center patch, and the feeding point is on the axis of symmetry. The structure parameters of antenna are calculated by theoretical formula of microstrip antenna, and impedance matching is realized by simulation and optimized in HFSS to make the characteristic parameters reach the maximum. Table 1 summarizes detailed dimensions of the proposed structure. SMV1247 and SMV1281 varactor diodes are selected due to their low series resistance and adequate range of junction capacitance from $0.64 \sim 8.86$ pF and $0.69 \sim 13.3$ pF. The equivalent circuit modes of varactor diode and its model used in the simulation software (HFSS) are illustrated in Figure 2. Source Meter is used to provide variable bias voltages for varactor diodes.

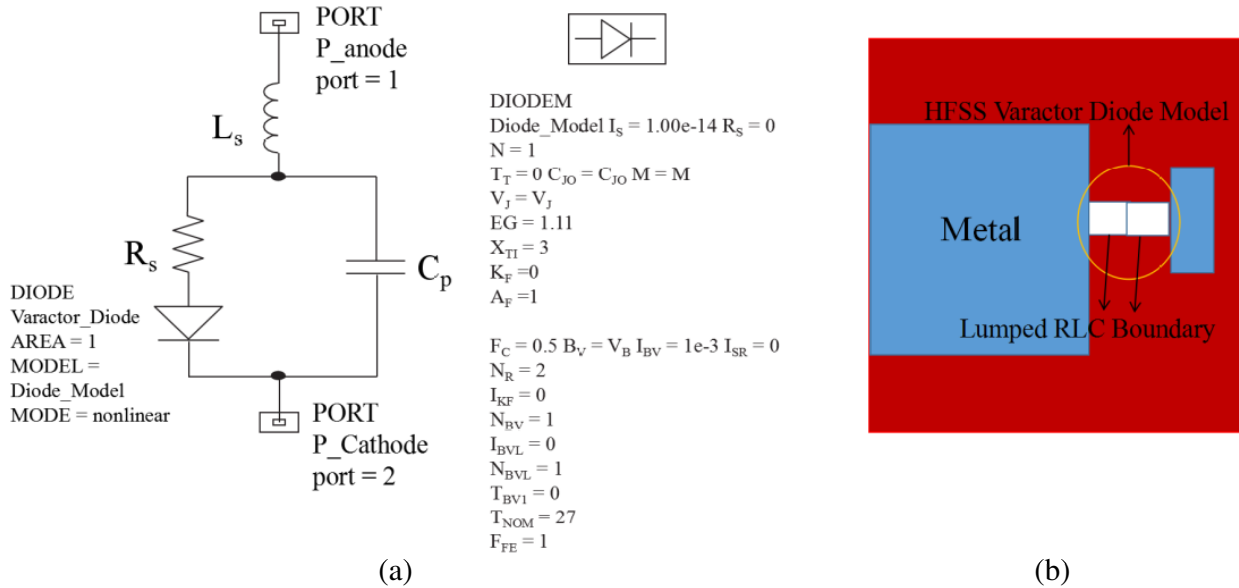


Figure 2. Electrical model of varactor diode: (a) Equivalent lumped element model, (b) simulation model in HFSS.

Table 1. Optimized size of the proposed antenna.

Parameter	Values (mm)
L	16.95
W	19
L_1	3.39
L_0	5
W_0	2

2.2. Reconfigurability Mechanism and DC Bias Network

Firstly, a microstrip patch antenna with a resonant frequency in 4 GHz is obtained by optimizing the size of the center rectangular patch and the position of the feeding point, giving rise to the tunable range of the antenna covering S-band and C-band. Then, parasitic patches are added in the center direction of the edges, and the size of parasitic patches is optimized to observe the return loss of the antenna from 2 to 8 GHz. It is found that there exist two resonant frequencies in 3.72 GHz and 5.52 GHz, which fall into S and C bands, respectively. Finally, with aim at switchable resonant frequencies, certain IV operating performance of varactor diodes is subjected to an external DC bias voltage to guarantee continuous recolonization with a certain range.

When V_1 is added (State I), the capacitances of upper and lower varactor diodes along with the x -axis direction change simultaneously, and the resonant frequency is tunable in the S-band. At the same time, V_2 and V_3 exert no effect on it. When V_2 or V_3 is added separately (State II, State III) and the other voltage remains as the highest to make the capacitance as low as possible, the tunable range of the resonant frequency is almost the same in the C-band. It is because the antenna has a symmetrical structure, contributing to the same resonant frequency, equal amplitude, and phase of State II and State III. In addition, the coaxial feeding point is just on the axis of symmetry without any connection to the ground. According to the electric field distribution on the surface of the radiation patch, the electric field of two varactor diodes along the axis of symmetry is almost unaffected by the y -axis direction.

In the actual measurement, varactor diodes are divided into three groups. In order to investigate the effect of external bias voltage on the frequency spectrum of varactor diodes, three independent DC bias voltages (namely V_1 , V_2 , and V_3) are applied to patches separately. Figure 3 shows the biasing circuit for a varactor diode. Resistors and capacitors are placed to enervate the RF signal and isolate the DC in order to prevent excessive current from damaging the instrument.

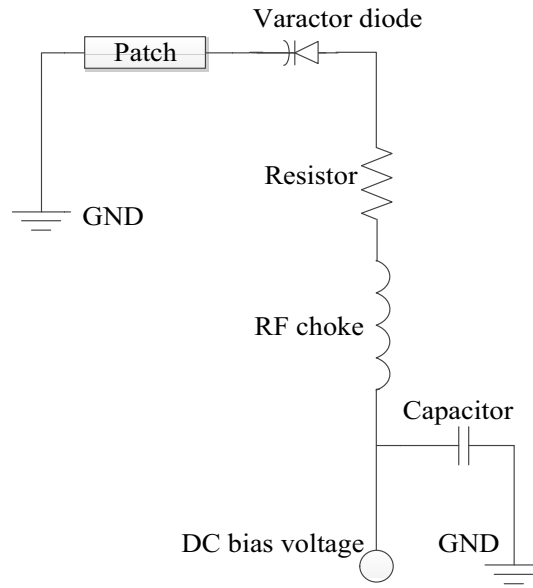


Figure 3. DC bias circuit of the varactor diode.

3. SIMULATED AND MEASURED RESULTS

The conductive gel is used to establish an electrical connection between varactor diodes and the patch. As displayed in Figure 4, the antenna is fabricated on an FR4 Substrate (dielectric constant $\epsilon_r = 4.4$, $\tan \delta = 0.02$) with a thickness of 1.6 mm. Simulation results are obtained using ANSYS High Frequency Structure Simulator (HFSS), and the return loss is measured by the Agilent N5230A vector network analyzer to verify the accuracy of the frequency reconfigurable antenna design.

3.1. Return Loss

The simulated and measured return losses for the antenna at S-band and C-band operating states under different bias voltages are illustrated in Figure 5 and Figure 6, respectively. The resonant frequency changes significantly for different DC bias voltages. This could be ascribed to that the E -field distribution is different at different bands as shown in Figure 7. Also noted in Figure 5, the antenna resonant frequency can be altered from 3.29 GHz to 4.01 GHz by varying the reversed bias voltage from 0 to 20 V. In Figure 6, the resonant frequency of the antenna can be changed from 5.35 to 7.00 GHz across the DC bias voltage from 0 to 8 V.

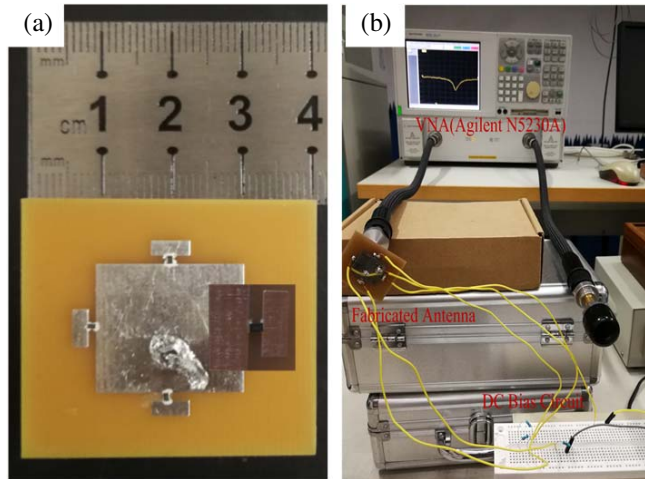


Figure 4. (a) Top view of the fabricated antenna, (b) experimental equipment for return loss measurement.

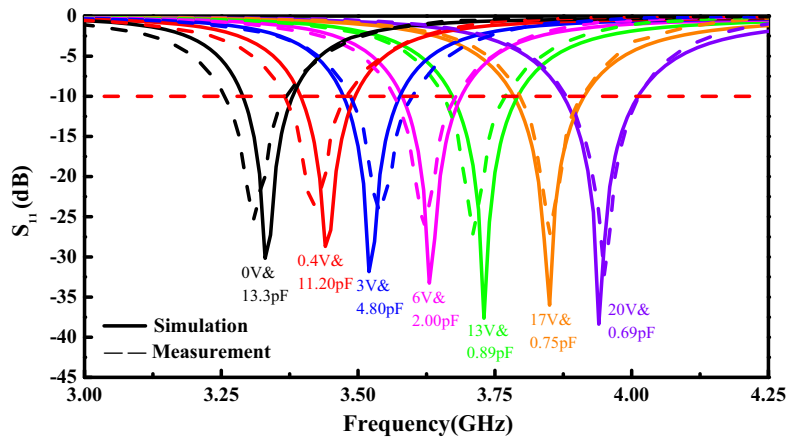


Figure 5. Dependence of return loss on DC bias voltage V_1 at S-band.

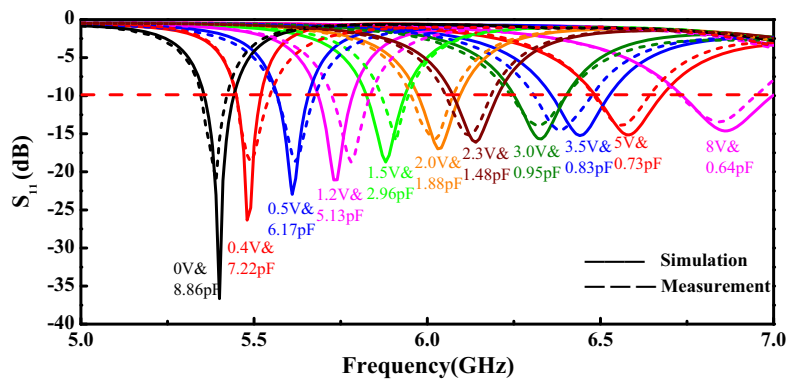


Figure 6. Dependence of return loss on DC bias voltage V_2 or V_3 at C-band.

It should be noted that resonant frequencies shift toward higher values with increase in bias voltage and decrease in capacitances. This phenomenon could be explained as follows. With the DC bias voltage increased, the capacitance of varactor diodes presents decreasing trend, giving rise to decreased equivalent electrical length of antenna. Consequently, the resonant frequency is inclined to shift towards

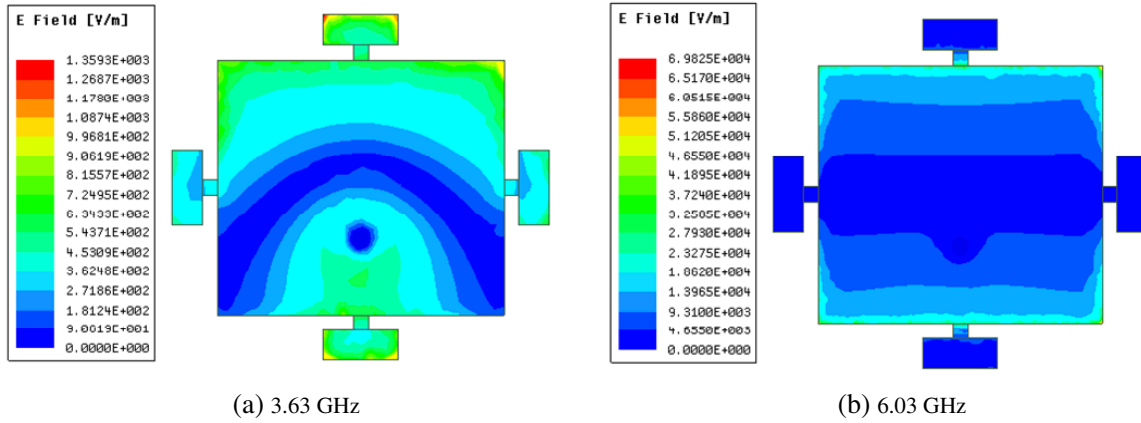


Figure 7. Simulated E field distribution of the antenna at (a) 3.63 GHz and (b) 6.03 GHz.

higher range. For all tunable frequencies, the return loss is less than -10 dB. It should be pointed out that there is a slight difference between the measurement and simulation due to fabrication inaccuracies and small measurement errors. In addition, the losses from varactor diodes cannot be exactly modeled in HFSS.

3.2. Radiation Pattern and Gain

Figure 8 demonstrates simulated radiation patterns in both E -plane and H -plane at typical different center frequencies of 3.52, 3.94, 5.48, 6.03, 6.33, and 6.86 GHz. Radiation patterns maintain similar shapes throughout the entire frequency band because the structures are very similar at different states. Additionally, the maximum gain radiation direction of the E -plane and H -plane is around 0° . In short, the proposed antenna is unidirectional, and the radiation pattern is stable within a wide frequency

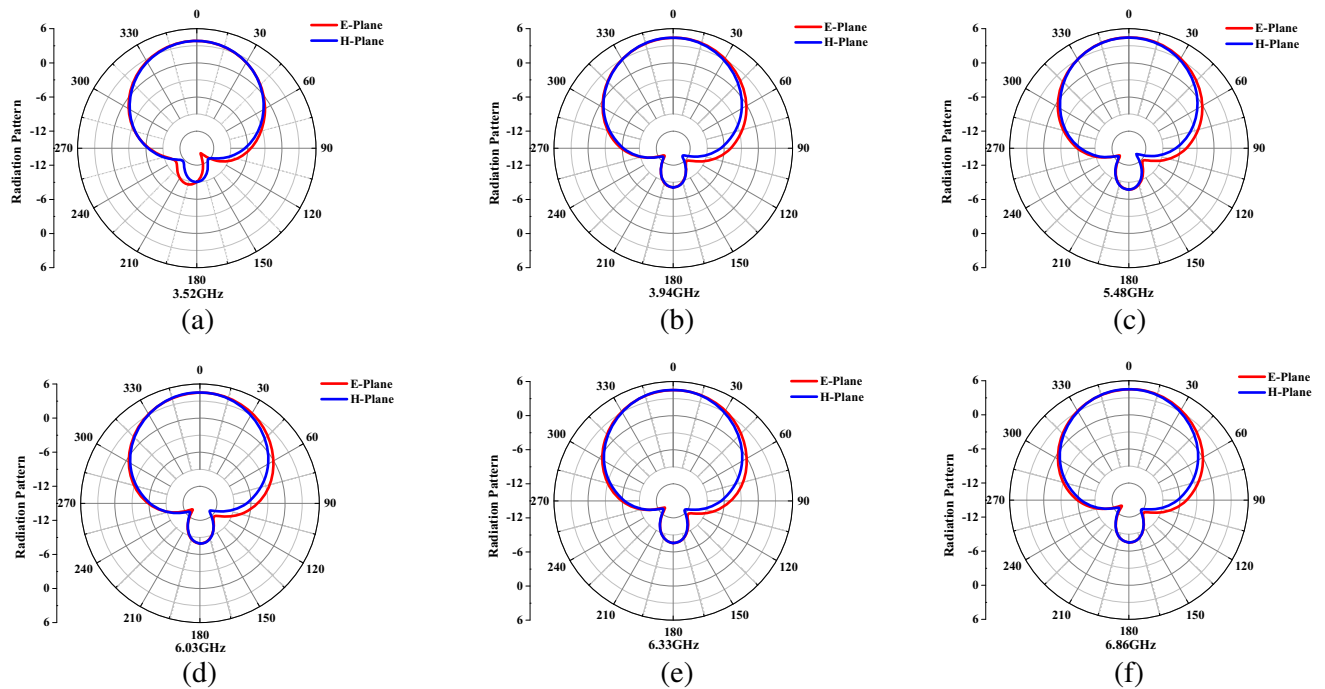


Figure 8. Simulated radiation patterns of the proposed antenna in both E -plane and H -plane at several center resonant frequencies: (a) 3.52 GHz, (b) 3.94 GHz, (c) 5.48 GHz, (d) 6.03 GHz, (e) 6.33 GHz, and (f) 6.86 GHz.

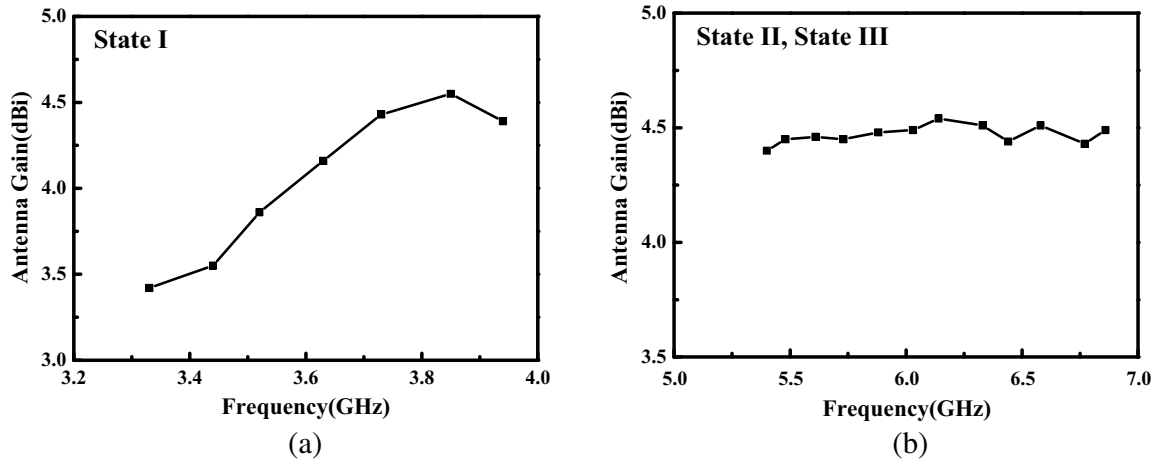


Figure 9. Simulated gain versus frequency of the proposed antenna.

range.

Additionally, gains at different resonant frequencies under different DC bias voltages are also displayed in Figure 9. At low frequencies, the capacitance of varactor diodes is larger when DC bias voltages are lower, and it makes the current loss increase at high capacitance levels, which leads to lower gains. However, gains are maintained at about 4.5 dBi in other tunable ranges, which are satisfactory for the monopole antenna in the intended applications. The overall performance of the proposed antenna satisfies requirements of the wireless communication system.

However, gains are maintained at about 4.5 dBi in other tunable ranges, which are satisfactory for the monopole antenna in the intended applications. The comparison of performance in our work with previous work is summarized in Table 2. It reveals that the proposed antenna has two operating bands with a smaller size and more stable gain. In addition to its compact size and four varactor diodes, the proposed antenna shows better performance in terms of wider range of reconfigurable frequency. Furthermore, the structure of the proposed antenna is simple, in low cost, and easy to fabricate.

Table 2. Performance comparison of the proposed antenna with the previous works.

Ref.	Type	Size (mm ³)	No. of Diodes	Frequency Tunable Ranges	Gain (dBi)
[24]	disperse	50 × 50 × 3.04	5	S-band (1.98 ~ 3.59 GHz)	0.20 ~ 4.80
[25]	continuous	70 × 70 × 2.0	2	S-band (2.45 ~ 3.55 GHz)	4.25 ~ 8.49
[26]	continuous	80 × 80 × 2.4	2	S-band (3.50 ~ 3.90 GHz)	3.80 ~ 6.00
This work	continuous	33.9 × 38 × 1.6	4	S-band (3.29 ~ 4.01 GHz)	4.50
				C-band (5.35 ~ 7.00 GHz)	

4. CONCLUSION

A frequency continuous tunable microstrip antenna tunable covering S-band and C-band is successfully designed and experimentally validated during fabrication and measurement. Four varactor diodes loaded on the radiation patch in a symmetrical distribution with three DC biasing voltages are used to control the frequency reconfigurability of the designed antenna. The effects of DC bias voltage on the reflection loss, radiation pattern, and gain are investigated from both simulated and experimental points of view. The measured results of return loss within frequency tunable ranges agree well with simulations. In addition, the proposed antenna obtains two tunable ranges and a stable gain radiation pattern about 4.5 dBi. The low profile, compact size, good frequency reconfiguration, and stable unidirectional radiation pattern of the antenna render it suitable for a wireless communication system.

ACKNOWLEDGMENT

This work was supported in part by the National Key Research and Development Program of China (Grant No. 2017YFA0204600), the National Natural Science Foundation of China (Grant No. 51802352), and the Fundamental Research Funds for the Central Universities of Central South University (No. 2018zzts355).

REFERENCES

1. Sboui, L., Z. Rezki, A. Sultan, and M. S. Alouini, "A new relation between energy efficiency and spectral efficiency in wireless communications systems," *IEEE Wireless Communications*, Vol. 26, No. 3, 168–174, 2019.
2. Zhou, L., J. Rodrigues, H. Wang, M. G. Martini, and V. Leung, "5G multimedia communications: Theory, technology, and application," *IEEE Multimedia*, Vol. 26, No. 1, 8–9, 2019.
3. Balasubramaniam, S., S. A. Wirdatmadja, M. T. Barros, Y. Koucheryavy, and J. M. Jornet, "Wireless communications for optogenetics-based brain stimulation: Present technology and future challenges," *IEEE Communications Magazine*, Vol. 56, No. 7, 218–224, 2018.
4. Chattha, H. T., M. Hanif, X. Yang, I. E. Rana, and Q. H. Abbasi, "Frequency reconfigurable patch antenna for 4G LTE applications," *Progress In Electromagnetics Research M*, Vol. 69, 1–13, 2018.
5. Chen, Y., B. Ai, Y. Niu, R. He, and Z. Han, "Resource allocation for device-to-device communications in multi-cell multi-band heterogeneous cellular networks," *IEEE Transactions on Vehicular Technology*, Vol. 68, No. 5, 4760–4773, 2019.
6. Björn, T., T. Arno, F. Jonas, C. Davide, T. R. Christer, V. Günter, M. Luc, and J. Wout, "Radio frequency electromagnetic field compliance assessment of multi-band and MIMO equipped radio base stations," *Bioelectromagnetics*, Vol. 35, No. 4, 296–308, 2014.
7. Tamagnone, M., J. S. G. Diaz, J. R. Mosig, and J. Perruisseau-carrier, "Reconfigurable THz plasmonic antenna concept using a graphene stack," *Applied Physics Letters*, Vol. 101, No. 21, 836–842, 2012.
8. Piazza, D. and K. R. Dandekar, "Reconfigurable antenna solution for MIMO-OFDM systems," *Electronics Letters*, Vol. 42, No. 8, 446, 2006.
9. Senanayake, R., P. J. Smith, P. A. Martin, and J. S. Evans, "Performance analysis of reconfigurable antenna arrays," *IEEE Transactions on Communications*, Vol. 65, No. 6, 2726–2739, 2017.
10. Tian, W., D. Wu, Q. Chao, Z. Chen, and Y. Wang, "Application of genetic algorithm in $M \times N$ reconfigurable antenna array based on RF MEMS switches," *Modern Physics Letters B*, Vol. 32, No. 30, 585–702, 2018.
11. Zhou, Q. F., H. An, P. Min, F. Qu, and L. Fan, "On the mode switching of reconfigurable-antenna-based blind interference alignment," *IEEE Transactions on Vehicular Technology*, Vol. 66, No. 8, 6958–6968, 2017.
12. Yadav, A., M. Tewari, and R. P. Yadav, "Pixel shape ground inspired frequency reconfigurable antenna," *Progress In Electromagnetics Research C*, Vol. 89, 75–85, 2019.
13. Chaouche, Y. B., F. Bouttout, M. Nedil, I. Messaoudene, and I. Benmabrouk, "A frequency reconfigurable U-shaped antenna for dual-band WIMAX/WLAN systems," *Progress In Electromagnetics Research C*, Vol. 87, 63–71, 2018.
14. George, R., C. R. S. Kumar, S. Gangal, and M. Joshi, "Frequency reconfigurable pixel antenna with PIN diodes," *Progress In Electromagnetics Research Letters*, Vol. 86, 59–65, 2019.
15. Shirazi, M., J. Huang, T. Li, and G. Xun, "A switchable-frequency slot-ring antenna element for designing a reconfigurable array," *IEEE Antennas & Wireless Propagation Letters*, Vol. 17, No. 2, 229–233, 2017.
16. Bharathi, A., M. Lakshminarayana, and P. V. D. S. Rao, "A quad-polarization and frequency reconfigurable square ring slot loaded microstrip patch antenna for WLAN applications," *AEU — International Journal of Electronics and Communications*, Vol. 78, 15–23, 2017.

17. Nafde, Y. and R. Pande, "Design and analysis of resistive series RF MEMS switches based fractal U-slot reconfigurable antenna," *Wireless Personal Communications*, Vol. 97, No. 12, 1–16, 2017.
18. Nguyen-Trong, N., L. Hall, and C. Fumeaux, "A frequency- and polarization-reconfigurable stub-loaded microstrip patch antenna," *IEEE Transactions on Antennas & Propagation*, Vol. 63, No. 11, 5235–5240, 2015.
19. Ullah, S., S. A. A. Shah, M. F. Khan, S. Ullah, and J. A. Flint, "Design of a multi-band frequency reconfigurable planar monopole antenna using truncated ground plane for Wi-Fi, WLAN and WiMAX applications," *ICOSST 2014*, 2014,
20. Tong, L., H. Zhai, W. Xin, L. Long, and C. Liang, "Frequency-reconfigurable bow-tie antenna for bluetooth, WiMAX, and WLAN applications," *IEEE Antennas & Wireless Propagation Letters*, Vol. 14, 171–174, 2015.
21. Haraz, O. M., S. A. Alshebeili, and A. R. Sebak, "Low-cost high gain printed log-periodic dipole array antenna with dielectric lenses for V-band applications," *Microwaves Antennas & Propagation, IET*, Vol. 9, No. 6, 541–552, 2015.
22. Cai, Y. M., S. Gao, Y. Yin, W. Li, and Q. Luo, "Compact-size low-profile wideband circularly polarized omnidirectional patch antenna with reconfigurable polarizations," *IEEE Transactions on Antennas & Propagation*, Vol. 64, No. 5, 2016–2021, 2016.
23. Sato, S., S. Saito, and Y. Kimura, "A frequency tunable ring microstrip antenna fed by an L-probe with varactor diodes," *2015 IEEE International Symposium on Antennas and Propagation & USNC/URSI National Radio Science Meeting*, 2015,
24. Majid, H. A., M. K. A. Rahim, M. R. Hamid, N. A. Murad, and M. F. Ismail, "Frequency-reconfigurable microstrip patch-slot antenna," *IEEE Antennas & Wireless Propagation Letters*, Vol. 12, No. 1921, 218–220, 2013.
25. Cai, Y., K. Li, Y. Yin, S. Gao, W. Hu, and L. Zhao, "A low-profile frequency reconfigurable grid-slotted patch antenna," *IEEE Access*, Vol. 6, 36305–36312, 2018.
26. Tateno, H., S. Saito, and Y. Kimura, "A frequency-tunable varactor-loaded single-layer ring microstrip antenna with a bias circuit on the backside of the ground plane," *2016 IEEE International Symposium on Antennas and Propagation & USNC/URSI National Radio Science Meeting*, 2016.